

What Makes Good Synthetic Training Data for Zero-Shot Stereo Matching?

David Yan
Princeton University
yan.david@princeton.edu

Alexander Raistrick
Princeton University
araistrick@princeton.edu

Jia Deng
Princeton University
jiadeng@princeton.edu

Abstract

Synthetic datasets are a crucial ingredient for training stereo matching networks, but the question of what makes a stereo dataset effective remains underexplored. We investigate the design space of synthetic datasets by varying the parameters of a procedural dataset generator, and report the effects on zero-shot stereo matching performance using standard benchmarks. We validate our findings by collecting the best settings and creating a large-scale dataset. Training only on this dataset achieves better performance than training on a mixture of widely used datasets, and is competitive with training on the FoundationStereo dataset, with the additional benefit of open-source generation code and an accompanying parameter analysis to enable further research. We open-source our system at [this URL](#) to enable further research on procedural stereo datasets.

1. Introduction

Synthetic data rendered by computer graphics is widely used for training models for stereo matching. Stereo matching uses a pair of RGB images to estimate per-pixel disparity, which can in turn be used to calculate scene depth. Synthetic datasets provide high-quality ground truth disparity calculated using depth from the rendering pipeline. State-of-the-art methods in stereo matching [5, 12, 17–19, 33, 35, 37, 38, 43–45] all train on synthetic datasets [4, 9, 19, 30, 32, 40]. Therefore, developing new synthetic datasets has been a significant component of recent work on stereo matching [17, 36].

Designing effective synthetic datasets remains a significant challenge. Existing synthetic stereo datasets vary significantly in their designs and realism, from random flying objects scattered in a scene [17, 19], to realistic domain-specific simulators [4, 9]. However, assessing *what matters in dataset design* is difficult because new datasets typically change many different factors at once. If an existing dataset is particularly helpful, was it because of the scene realism, object diversity, materials, or camera placement? The best choices are not obvious - more extreme arrangements could

either improve a model’s performance by making it more robust to a wider distribution, or could harm performance by diverging from real-world scenes in downstream tasks.

In this work, we systematically explore the design space of synthetic data for stereo matching using procedural generation. Procedural generation creates synthetic data using randomized computer graphics algorithms, which means the entire data generation process can be controlled and customized to investigate downstream performance.

We construct a procedural generator for stereo datasets by combining object- and scene-level generators from Infinigen [23, 24] with new features designed to support large-scale stereo dataset generation. To ensure good coverage of common stereo dataset designs, we add new placement generators for floating objects and random lighting. We also add tools to avoid problematic objects and materials, such as one that removes glass from subparts of objects. By varying the procedural parameters of this generator, we can analyze several common features of stereo datasets, including floating object density, background objects, object category, object materials, and augmented lighting, as well as the parameters of these features, e.g. the density of floating object placement, or which materials are used for augmentation.

We investigate which dataset designs lead to strong benchmark performance in zero-shot, that is, *without* any fine-tuning. For each parameter setting, we generate a stereo matching dataset, then train and evaluate a RAFT-Stereo model to determine the downstream effect on zero-shot performance. We evaluate in the zero-shot setting, similar to FoundationStereo [36] and StereoAnywhere [2], as it represents the typical off-the-shelf usage of a model. We aim to improve zero-shot performance on existing models by training on diverse synthetic data.

Our study yields a variety of interesting findings. Of all the designs tested, we found the most effective stereo data comes from the *combination* of realistic indoor scenes with added floating objects. Removing realistically arranged background furniture (leaving floating objects in empty rooms) or removing the entire background (leaving just floating objects) harms zero-shot generalization. We also find that existing stereo networks struggle to learn re-



Figure 1. **Visualization of synthetic dataset design choices.** For each studied parameter, we show a single illustrative example demonstrating the effect of changing dataset generation parameters such as object density, background realism, object types, lighting, and materials. Each example is sampled from a dataset evaluated in Tab. 1.

flective and transparent materials without large performance drops on diffuse regions. These results show that certain aspects of scene realism are helpful for zero-shot stereo, while also suggesting that scenes designed to be fully realistic lack sufficient dense geometry to be data-efficient.

We use the best discovered settings to create WMGStereo-150k, a new training dataset for stereo matching. Training on only this dataset produces better zero-shot results than training on SceneFlow [19], CREStereo [17], TartanAir [32], or IRS [31]. Moreover, training DLNR [45] on WMGStereo-150k outperforms training on the *combination* of these prior datasets by 28% on Middlebury [26] and by 25% on the Booster [25] evaluation sets (Tab. 2). We achieve competitive performance with the state-of-the-art dataset, FoundationStereo [36] (Tab. 5). Our dataset is also highly sample efficient: training on just 500 random examples from our dataset achieves lower error on Middlebury than 100,000 CREStereo examples (Fig. 5).

In summary, we make three main contributions. First, we provide a thorough analysis of the effects of common stereo dataset designs and possible parameter settings. Second, we provide WMGStereo-150k, a new large-scale dataset incorporating these findings. Finally, and uniquely among stereo datasets, our work provides procedural generation code, which we hope will be useful to generate additional data or enable further research to improve the usefulness of synthetic datasets for stereo matching.

2. Related Work

Synthetic Datasets for Stereo Matching Procedural datasets such as SceneFlow [19] typically use randomly placed flying objects with randomized backgrounds to

achieve high diversity. This procedural recipe for object placement remains highly effective, with procedural datasets such as CREStereo [17] and FallingThings [30] building upon the flying/floating object setup with additions such as photorealistic rendering and more diverse materials.

Non-procedural synthetic datasets [3, 21] such as IRS [31], TartanAir [32], UnrealStereo4k [29], and DynamicReplica [16] typically render frames from realistic scenes handcrafted by 3D artists. Simulators such as HS-VS [40] and VirtualKITTI [9] [4] primarily target driving scenarios.

Although these datasets have been widely adopted and have demonstrated success in state-of-the-art stereo networks, they do not report ablations over dataset generation parameters, and therefore provide limited insight into what actually makes these datasets so effective. Moreover, we cannot directly study generation parameters in existing datasets (e.g. re-rendering TartanAir with different materials) because they do not open-source their generation code or assets. We use the open-source Infinigen system to reproduce and analyze many existing design choices. We perform a detailed analysis of what parameters, such as object placement, camera parameters, and materials, matter most for downstream performance.

FoundationStereo [36] achieves state-of-the-art zero-shot performance by introducing a new model architecture alongside the FoundationStereo dataset (FSD). FSD adopts similar settings to our final dataset, such as combining floating objects with realistic background scenes and varying camera parameters. However, FoundationStereo does not provide any analysis of FSD or code to reproduce or expand its dataset. Our work provides this analysis and an open-source procedural generator to enable further research.

Procedural Generation Although there exist several

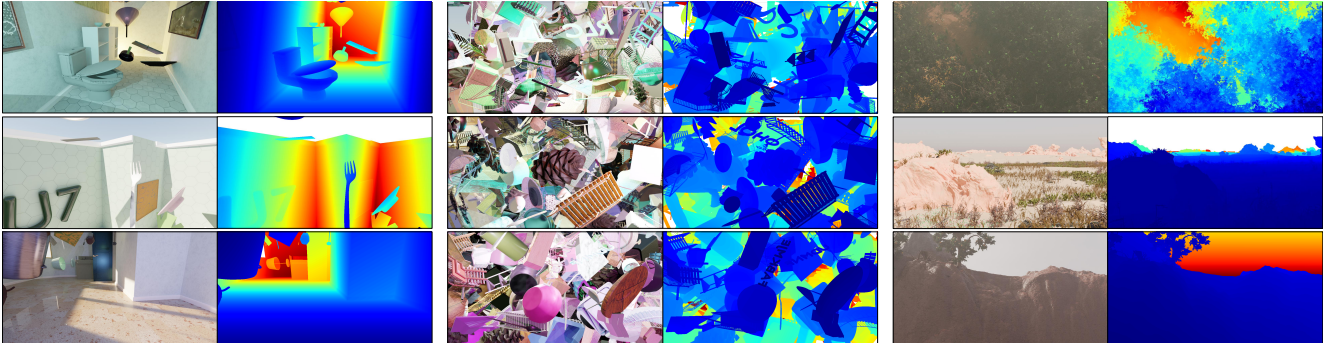


Figure 2. **WMGStereo-150k Dataset**. From left to right, we show random, non-cherrypicked samples from our *Indoors with Floating Objects*, *Dense Floating Objects*, and *Nature* scene types. Refer to the Supplement for additional samples.

open platforms for procedural data generation, there has been limited use of these platforms to produce large-scale stereo datasets. Kubric [11] generates scattered or falling objects in a 3D scene, while ProcTHOR [7] generates realistic indoor environments for embodied agent training. However, neither pipeline has demonstrated use in stereo matching. Infinigen Nature [23] and Infinigen Indoors [24] use Blender [6] to procedurally generate realistic indoor and natural scenes. Raistrick et al. [23] created a stereo dataset using Infinigen Nature, but it did not achieve competitive performance with SceneFlow. The Infinigen-SV [15] dataset only uses Infinigen Nature and focuses on augmenting SceneFlow for video-consistent stereo networks.

Our work significantly expands on the object and scene generators from Infinigen [23, 24]. We develop a procedural placement algorithm for floating object and lighting placement integrated with Infinigen scene and object generators. Our algorithm supports common features in stereo datasets and enables us to exercise fine-grained control over objects, materials, lighting, and cameras. For instance, we can remove different classes of objects from generation and even remove specific materials from individual objects. We open-source our configurations, enabling others to easily create targeted data, such as scenes with extreme clutter or all glass materials. Our dataset is a novel demonstration of general-purpose scene generators for stereo data.

Analysis of Synthetic Datasets Mayer et al. [20] perform a detailed study of the procedural generation parameters of synthetic training data for optical flow and disparity prediction. This study concludes that “realism is overrated” for effective synthetic data, motivating the further development of successful flow datasets such as AutoFlow [13, 28]. However, this study primarily studies generation parameters for FlyingChairs-style datasets [8, 14], which consist only of warped 2D images with no depth or disparity. Moreover, their study of disparity prediction focuses on augmentations simulating camera noise and blurring. As such, there is limited study of critical generation parameters, such as object

placement and realism, for modern stereo datasets rendered from 3D scenes. Our study focuses on stereo depth prediction, uses more realistic 3D procedural generators, and applies directly to modern stereo networks. We find that a mix of placement realism and random floating objects is an effective recipe for stereo data. While this result supports Mayer et al.’s conclusion that diversity from randomly scattered objects is important, it also suggests that scene realism can help significantly with zero-shot generalization.

3. Analysis of Dataset Parameters

3.1. Initial procedural generator

We construct our system on top of the Infinigen and Blender Python APIs. Infinigen provides high-level APIs to generate objects (e.g. chairs, plants, staircases) and scenes (indoor rooms, nature, or blank sky backgrounds). We directly use the Blender API to implement multiple new scene arrangement generators and other modifications that are specifically tailored to create effective stereo datasets.

Specifically, we create a floating object placement interface that calls the Infinigen API to generate objects and then arranges them throughout a given scene type. Our floating object placement has options to place objects in the view of a given camera through raycasting or to place objects within a specified bounding box. We also provide an option to allow floating objects to intersect existing scene geometry.

Our modifications to the Infinigen system and our floating object interface enable the system to generate three distinct scene types: indoor floating objects, dense floating objects, and nature. For the indoor floating objects scene type, we generate rooms from the Infinigen Indoors system and use our interface to generate objects at randomly sampled locations in the room. For the dense floating object scene type, we spawn a camera rig in an empty sky scene and use our interface to place objects within view of the camera. Nature scenes are generated from Infinigen Nature.

Experiment	Method	Middlebury 2014 (F)	Middlebury 2014 (H)	Middlebury 2021	ETH3D	KITTI-12	KITTI-15	Booster (Q)
Floating Object Density	No floating objects	18.44	12.52	16.31	4.47	4.42	6.19	16.40
	0 to 10 floating objects	11.42	7.78	11.30	3.62	4.44	6.09	12.21
	10 to 30 floating objects	9.19	6.60	10.28	3.92	4.05	5.11	10.60
Background Objects	No background objects	10.42	8.35	12.01	4.39	4.20	6.28	12.72
	With background objects	9.19	6.60	10.28	3.92	4.05	5.11	10.60
Floating Object Type	Floating chairs	9.24	5.29	9.81	3.64	4.90	7.02	11.22
	Floating shelves	10.28	7.13	10.24	3.51	4.32	6.06	11.63
	Floating bushes	9.20	6.04	9.53	3.13	3.86	5.42	12.19
	All generators used	9.19	6.60	10.28	3.92	4.05	5.11	10.60
Object Material	No materials	11.42	9.02	10.65	3.48	4.34	6.07	14.07
	One diffuse material	10.09	7.21	9.65	2.77	3.76	5.41	12.73
	Only metal and glass	11.28	8.37	11.85	4.95	4.06	4.97	9.80
	All materials used	9.19	6.60	10.28	3.92	4.05	5.11	10.60
Stereo Baseline	Uniform[0.04, 0.1]	32.47	9.60	22.18	2.89	5.13	6.64	17.03
	Uniform[0.2, 0.3]	9.75	7.01	10.50	14.05	3.94	5.37	8.96
	Uniform[0.04, 0.4]	9.19	6.60	10.28	3.92	4.05	5.11	10.60
Lighting	Realistic Lighting	9.62	6.91	10.06	3.81	3.95	5.45	10.45
	Augmented Lighting	9.19	6.60	10.28	3.92	4.05	5.11	10.60

Table 1. **Results of generation parameter study.** For each variation, we generate a new dataset of 5,000 stereo pairs and use it to train RAFT-Stereo [18]. We report the zero-shot performance on a variety of standard benchmarks. We bold the best-performing models and the settings chosen for our final generator.

3.2. Parameter Study

We perform a systematic study to determine the effect of procedural generation parameters on zero-shot stereo matching performance. For a variety of parameters, we directly evaluate their effect on zero-shot performance. In each such case, we generate 5000 stereo pairs using the indoor floating objects scene type. We show a single illustrative example of each dataset in Fig. 1. We train RAFT-Stereo [18] on each of these datasets for 75k steps using standard training settings. Finally, we evaluate the resulting models on the Middlebury [26], ETH3D [27], KITTI [10, 22], and Booster [25] datasets and report results in Tab. 1. This training setup uses less data and a shorter training schedule to enable fast experimentation. In practice, we find that this reduced scale is sufficiently representative of the full-scale training runs.

We evaluate zero-shot performance on the Middlebury 2014 evaluation set, the Middlebury 2021 dataset, the ETH3D train set, the KITTI 2012 and KITTI 2015 train sets, and the Booster train set. For each dataset, px error is defined as the percentage of pixels with end-point-error exceeding a specified threshold. The thresholds are chosen using standard ranking metrics: 2px non-occluded error for Middlebury 2014, 2px error for Middlebury 2021, 1px error on ETH3D, 3px error for KITTI 2012 and KITTI 2015, and 2px error on Booster. We evaluate on full (F) and half (H) resolution on Middlebury and on quarter (Q) resolution on Booster.

Floating Object Density. Floating objects (or flying ob-

jects) are a common feature of stereo datasets. However, it is plausible that realistically arranged objects such as those produced by Infinigen Indoors would be better aligned with the distribution of real-world scenes. First, we validate whether adding floating objects to scenes that already contain realistic room layouts provides any benefit. We compare scenes with either no floating objects or 0 to 10 floating objects, and confirm that this improves Middlebury 2014 (H) 2px error (12.52 to 7.78). Next, we compare this to a setting with far greater density of floating objects (uniformly sampled from 10 to 30 per scene) and again find a 2px error improvement (7.78 to 6.60). This confirms that floating objects are extremely helpful for zero-shot performance, despite resulting in less realistic scenes. Following this result, we place 200 objects in our dense floating object scenes to maximize object density.

Background Objects. Next, we investigate whether the furniture and other background objects (e.g. shelves, tables) which appear in indoor scenes are useful. Such arranged objects are not present in other procedural datasets like FlyingThings3D, and previous studies indicate that realism, such as these realistically placed objects, is not important [20]. However, when evaluating scenes with and without background objects, we find that including background objects *does* help, improving performance on all benchmarks (e.g. 8.35 to 6.60 2px error on Middlebury 2014 (H)).

Object Type. We investigate to what extent the diversity of objects is useful: how helpful is sampling from all available Infinigen object generators, as opposed to using only a single class of objects? We find that using only chairs results

Model	Middlebury 2014 (H)	Middlebury 2021	ETH3D	KITTI		Booster (Q)
				2012	2015	
PSMNet [5]	13.80	23.67	19.75	6.73	6.78	34.47
RAFT-Stereo [18]	8.66	10.28	2.6	4.35	5.67	17.37
IGEV [37]	11.81	20.43	43.05	7.62	7.81	23.38
GMStereo [39]	10.98	25.43	6.22	5.68	5.72	32.44
DLNR [45]	6.20	8.44	23.01	9.08	16.05	18.15
Selective-IGEV [33]	7.30	8.97	6.07	5.64	6.05	17.58
NMRF [12]	10.87	23.36	4.34	4.62	5.24	27.08
IGEV++ [38]	7.75	9.58	4.67	6.23	6.40	17.22
StereoAnywhere [2]	4.75	5.71	1.43	3.52	3.79	9.01
FoundationStereo [36]	1.10	4.17	0.50	2.30	2.80	4.16
RAFT-Mixed	5.50	8.97	2.58	3.64	4.95	11.46
RAFT-WMGStereo-150k	4.48	8.17	2.93	3.25	4.25	9.17
Selective-IGEV-Mixed	5.24	8.24	2.37	3.97	5.31	11.00
Selective-IGEV-WMGStereo-150k	3.61	7.62	2.47	3.26	4.55	8.84
DLNR-Mixed	5.21	9.30	2.50	3.68	4.95	12.17
DLNR-WMGStereo-150k	3.76	6.72	2.50	3.30	4.54	9.09

Table 2. **Zero-shot stereo results** Models trained on WMGStereo-150k outperform many prior methods (top section) on zero-shot stereo matching for standard benchmarks. Mixed is a combined synthetic dataset of SceneFlow, CREStereo, TartanAir, and IRS (600k total pairs). Training on our dataset yields improvements for many stereo models, demonstrating that our findings generalize across architectures. Although our models perform worse than FoundationStereo, which is significantly larger than our retrained models, we achieve competitive performance with StereoAnywhere, a recent model focused on zero-shot stereo with similar computational cost to our tested architectures.

in small improvements on some benchmarks (Middlebury 2014 and 2021). Fixing the object type to shelves results in worse performance on all benchmarks except ETH3D. Meanwhile, using only the bush object type leads to better performance on KITTI-12 and ETH3D. These results likely reflect the biases of individual benchmarks toward certain object types. For instance, one can improve performance on indoor benchmarks (6.60 to 5.29 2px error on Middlebury 2014 (H)) by using only chairs, but at the cost of significantly worse performance on driving scenarios (5.11 to 7.02 3px error on KITTI-15). Meanwhile, using only bushes helps on benchmarks like KITTI-12 and ETH3D (3.92 to 3.13 1px error), which have more nature coverage but hurts performance on Booster (10.60 to 12.19 2px error), which focuses on specular and indoor scenes. As such, we choose to use all generators because it has the most robust performance across many benchmarks.

We also investigated objects at the level of individual object types and per-pixel errors. Specifically, we test a trained model on 1000 additional images rendered from the same procedural parameters, and we use object segmentation masks to compute average end-point-error aggregated across each object type. We plot the objects with the highest remaining error in Fig. 3. We manually inspected error maps for the highest error objects, and found objects such as cacti and urchins, which have very thin needle structures,

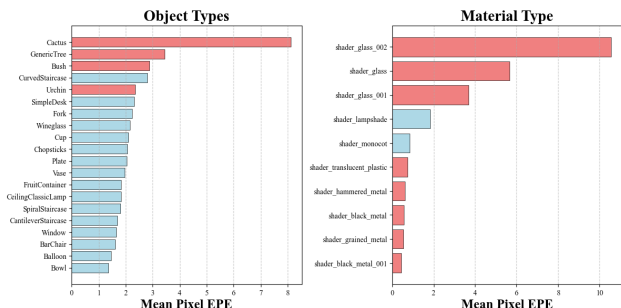


Figure 3. **End-point-error averaged by object and material.** We show average error only for the materials that make up at least 0.1% of pixels. Assets marked in red were removed from our system after manual inspection because they introduce ambiguous high-error cases, such as entirely transparent or reflective surfaces, or thin imperceptible foliage / holes.

and racks, which have very small holes. We remove these objects from our final system due to their extreme difficulty.

Object Materials. We investigate the impact of various categories of materials. We applied changes to all objects except the walls to prevent very ill-posed cases such as transparent or mirror-like walls. When only glass and metallic materials are used, the model achieves the best performance on KITTI-15 and Booster, likely because these benchmarks

feature many transparent or reflective surfaces. However, it has significantly worse performance on Middlebury and ETH3D. When using just a single diffuse material such as wood, the model obtains the best performance on Middlebury 2021, ETH3D, and KITTI-12, but does poorly on Booster, likely because of the lack of glass/metal coverage in the training data. When using no materials at all, the model performs worse across all benchmarks except ETH3D. Using a diverse array of materials results in the most robust performance across all benchmarks.

Similarly to object types, we also group per-pixel EPE by material and plot the materials with the highest error in Fig. 3. We limit this analysis to materials which comprise at least 0.1% of pixels, to prevent very rare materials (e.g. creature’s tongue / eyeball) from dominating the statistics due to low sample count. Eight of the ten highest errors are troublesome versions of glass and metal, which are often completely transparent or completely reflective. We remove these specific materials from our system, because we find current stereo networks struggle to handle ill-posed surfaces without degrading performance on diffuse regions. However, we retain many other non-Lambertian materials which are only moderately transparent/reflective. We take particular care for external windows - replacing the glass material for these with an opaque surface would ruin lighting for the rest of the scene, so we instead automatically delete the geometry to eliminate it from the ground truth.

Lighting Augmentation. We perform a suite of different lighting augmentations. We randomly place 0 to 5 point lights in the scene, with a total power sampled uniformly from 250 to 1250. We also randomly remove the ceiling with probability 0.3 to allow occasional natural sky lighting, and randomly dim the ceiling lights and alter their colors with probability 0.2 to cover darker scenes.

We found that lighting augmentation had little effect on benchmark performance, with some improvements on Middlebury 2014 and KITTI-15, and slightly worse performance on ETH3D, Middlebury 2021, and KITTI-12. It is plausible that the lack of difference is caused by insufficient lighting variation in the benchmarks. We opt to include augmented lighting in our dataset to better account for diverse, in-the-wild lighting variations.

Stereo baseline randomization. We find that having a wide range of camera baseline values is very significant for robust generalization. When trained only on small baselines uniformly sampled between 0.04 and 0.1 m, the model performs significantly worse across all benchmarks except ETH3D. When trained only on large baselines sampled between 0.2 and 0.3 m, the model’s performance improves on certain large disparity benchmarks such as Booster, but fails on small disparity benchmarks such as ETH3D. We choose to sample the baseline value uniformly from 0.04 to 0.4 m, which had the best performance.

Data Mix	Middlebury 2014		Middlebury 2021	ETH3D	KITTI	
	(F)	(H)			12	15
Indoor Floating	9.19	6.60	10.28	3.92	4.05	5.11
Dense Floating	15.25	9.90	12.25	3.40	7.22	9.13
Nature	18.61	12.27	16.92	4.23	6.24	7.74
Mixed Dataset	7.81	6.04	9.29	2.51	3.54	5.12
10 - 80 - 10	10.52	6.09	10.05	2.66	3.79	4.86
80 - 10 - 10	8.13	5.90	9.21	3.01	3.81	5.31
10 - 10 - 80	9.70	7.14	10.63	2.79	3.83	5.50
33 - 33 - 33	7.81	6.04	9.29	2.51	3.54	5.12

Table 3. **Performance of different data distributions.** Top half: individual scene types. Bottom half: different weightings of scene types. Mixed denotes a dataset of equal parts indoors, dense floating. Each label denotes % Indoor - % Dense Floating - %Nature data. A mixed dataset of all dataset types is the most effective, while the indoor floating type is the best individual data type.

Ratio of scene types. In Tab. 3, we experiment on the distribution of scene types using the same experimental setup of a 5k stereo pair budget and training RAFT-Stereo for 75k steps. We find that a mixed dataset of all scene types is the most effective for stereo generalization. We also observe that indoor floating object scenes are the best individual scene type on all benchmarks except ETH3D. This result verifies the effectiveness of combining realistic scenes with floating objects over random flying objects without a background. The dense floating object dataset likely performs better on ETH3D because it has lower average disparity values and more closely matches the benchmark’s distribution.

3.3. Data Generation Cost Optimization

Generating data with the default Infinigen configurations is computationally expensive. The two largest costs are CPU time for generating the scene, and GPU time for rendering images from the generated scene, which we aim to reduce.

Experiment	Midd-2014		Midd 2021	ETH3D	KITTI	
	(F)	(H)			12	15
<i>Ray-tracing Samples</i>						
8192	8.78	6.09	9.61	3.69	9.09	10.69
1024	9.06	6.90	10.54	4.17	7.86	8.60
1024 + denoise	9.19	6.60	10.28	3.92	4.05	5.11
1024 + denoise [†] (Ours)	7.92	5.63	9.88	2.91	3.62	5.45
<i>Solver Realism</i>						
Full Solve	9.90	6.15	9.76	3.19	4.23	6.29
Reduced Solve	9.19	6.60	10.28	3.92	4.05	5.11
Reduced Solve [†] (Ours)	7.92	5.63	9.88	2.91	3.62	5.45

Table 4. **Cost optimization study.** We use the same experimental setup as Tab. 1 except for those labeled with †, which denotes the generation *compute-matched* setting. Since our optimizations yield a 6× speedup, † corresponds to 30k samples instead of 5k. While these optimizations reduce performance, they lower dataset cost and lead to better performance in the fixed-compute regime.

Indoor arrangement quality. Infinigen’s room solver uses a simulated annealing algorithm that iteratively adds, removes, and moves objects to optimize a set of realism con-

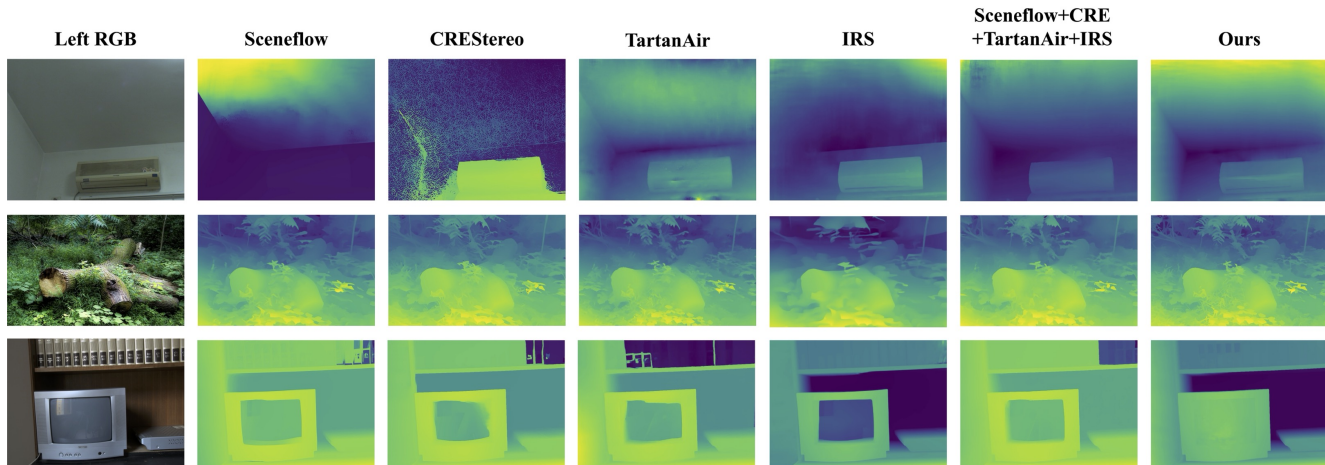


Figure 4. **Qualitative comparison of in-the-wild predictions.** We train DLNR on WMGStereo-150k and existing synthetic datasets. Training on our dataset achieves superior predictions on textureless regions (top row; blank ceiling), nature details (middle row; background leaves) and non-Lambertian surfaces (bottom row; TV screen). Images are from InStereo2k [1], Flickr1024 [34], and Booster [25].

straints. This process is slow, taking on average 50.85 minutes per indoor scene on 4 Xeon Gold 5320 CPUs. Naively reducing solver step count results in significantly sparser scenes, since the solver has fewer steps to place objects. We therefore constrain the solver to greedily add objects, which prevents the solver from wasting steps on moving and removing objects. This approach allows for significantly faster generation of densely populated scenes, at the cost of less realistic placement. We decrease the number of solver steps from 550 to 60, which reduces generation times to an average of 13 minutes. We observe that reducing solver realism leads to performance drops on Middlebury2014-H, Middlebury2021, and ETH3D, but not KITTI (Tab. 4). This result suggests that more regular and realistic background scenes may help with in-domain performance, but hurt out-of-domain generalization. In the fixed-compute setting, our low-cost settings achieve better or comparable performance.

Ray-tracing quality. Reducing sample count will linearly decrease render time, but results in high amounts of render noise in images. We propose the use of Blender’s OptiX denoising algorithm to mitigate render noise. The denoising process results in reduced render fidelity and occasional artifacts, but our experimentation demonstrates that it is effective at improving the trade-off between render speed and render quality. We set render samples to 1024, which reduces rendering time to just 27 seconds per frame.

We observe that, without denoising, higher render sample counts result in improved performance on all benchmarks except KITTI, suggesting that improved render quality generally improves performance (Tab. 4). We hypothesize that the large amounts of render noise function as an aggressive augmentation that aids generalization to the noisier images in the KITTI benchmark, but hurts performance

on domains which have cleaner captures. This is similar to findings in [20], which reports small performance on KITTI benefits from explicitly modeling interpolation artifacts. By applying denoising to low-sample renders, model performance generally improves across most benchmarks, demonstrating that render denoising is effective at mitigating performance losses caused by excessive render noise.

Scene generation amortization. To reduce CPU cost, we aim to render more frames from each scene without sacrificing diversity. Traditionally, stereo datasets render *video* trajectories from scenes. However, video sequences contain less diversity due to high overlap between nearby frames. Because we focus on two-view stereo matching, we achieve maximum diversity when frames are not contiguous. In each indoor scene, we place 20 separate stereo rigs, maximizing the standard deviation of depth values. For each dense floating object scene, we randomize object positions and orientations, lighting, and camera rig baseline values 200 times per scene. This allows us to generate fewer scenes, reducing CPU cost with a minimal loss in diversity.

4. WMGStereo-150k Dataset

We use the best settings in Tab. 1 to construct WMGStereo-150k, a stereo dataset of 163,666 stereo pairs. This dataset incorporates all the best parameter configurations found in Sec. 3. We include three categories of rendered scenes, shown in Fig. 2: indoor floating objects (71,947 stereo pairs), dense floating objects (70,300 stereo pairs), and nature scenes (21,419 stereo pairs).

The total data generation cost was approximately 70.5 days on 4 CPUs for scene generation and 120 GPU days for rendering. Without any optimizations, it would have taken 275 days on 4 CPUs and 900 days on 1 GPU. In practice, we

Dataset	Middlebury 2014		Middlebury 2021	ETH3D	KITTI		Booster (Q)
	(F)	(H)			2012	2015	
SceneFlow	10.96	6.20	8.44	23.12	9.45	15.74	18.17
CREStereo	14.45	11.53	10.6	5.18	4.95	5.90	14.61
TartanAir	12.56	7.27	14.47	4.35	3.98	5.33	18.14
IRS	7.81	6.13	8.49	3.91	4.56	5.60	10.32
WMGStereo-150k	5.10	3.76	6.72	2.50	3.30	4.54	9.09
FoundationStereo	<u>5.80</u>	3.27	<u>6.93</u>	2.13	<u>3.56</u>	4.18	7.51

Table 5. **Zero-shot performance by dataset.** DLNR trained only on WMGStereo-150k outperforms the same model trained on widely used stereo matching training datasets, and is competitive with training on the FoundationStereo dataset.

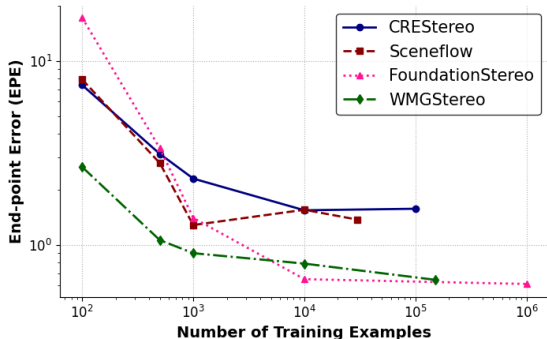


Figure 5. **Zero-shot performance by dataset size.** Our dataset is more *sample-efficient* than SceneFlow and CREStereo, achieving better performance across a range of dataset sizes. Our dataset achieves competitive performance with FSD.

parallelize these computations over many CPUs and GPUs, drastically reducing wall-clock time to generate the dataset.

We train RAFT-Stereo [18], DLNR [45], and Selective-IGEV [33] on our dataset for 200k steps, following the standard training procedures and hyperparameters used by the original authors. During training, we reweight the scene types on our dataset such that each type is sampled equally, following the results from the study in Section 3. During training, we mask the sky and the untextured room exteriors. We empirically found this to provide a small performance boost.

4.1. Zero-shot Generalization

Tab. 2 shows quantitative results for public models. Because most existing models are pre-trained only on SceneFlow, we retrain them on a mix of SceneFlow, TartanAir, CREStereo, and IRS to provide a more robust baseline (denoted -Mixed). DLNR-WMGStereo-150k outperforms DLNR-Mixed by 28% on Middlebury and by 25% on the Booster Benchmark. RAFT-WMGStereo-150k outperforms RAFT-Mixed by 11% on KITTI 2012 and by 14% on KITTI 2015, while Selective-IGEV-WMGStereo-150k

outperforms Selective-IGEV-Mixed by 20% on Booster. Notably, RAFT-WMGStereo-150k outperforms StereoAny-where on Middlebury 2014, despite not leveraging any large monocular depth priors such as DepthAnythingV2 [42].

4.2. Qualitative Results

In Fig. 4, we compare the qualitative results of a DLNR model trained on our dataset to the same model trained on other synthetic datasets. In the first row, we observe that our model accurately predicts difficult textureless regions. In the second row, our model is able to recover fine details from a natural scene, demonstrating that our model has not overfit to indoor domains. The third row shows that our model is robust to specular regions, likely due to WMGStereo-150k’s photorealistic rendering and lighting.

4.3. Dataset Comparison

We also compare our dataset individually to existing datasets. For each of SceneFlow, CREStereo, TartanAir, and IRS, we train DLNR for 200k steps using default training settings. We report quantitative zero-shot results in Tab. 5, using metrics as defined in Sec. 3. The model trained on WMGStereo-150k achieves better performance than classic datasets, with a 39% improvement over IRS on Middlebury 2014 (H), and is competitive with FSD. Despite not explicitly modeling driving scenarios like SceneFlow and FoundationStereo, our dataset achieves better performance than both datasets on KITTI-12. To demonstrate that our dataset has not overfit to the benchmarks in the study, we also evaluate on held out benchmarks not used in parameter tuning in Tab. 6. We use the Middlebury 2014 training set, excluding the standard 10 validation scenes, and a fixed, randomly selected subsample of 200 stereo pairs from the DrivingStereo [41] dataset.

We also demonstrate in Fig. 5 that our data is sample-efficient. Given a fixed dataset size, we train DLNR for 200k steps on WMGStereo-150k, SceneFlow, and CREStereo and evaluate their zero-shot performance on end-point error (EPE) on Middlebury 2014 (H). We find that just 500 training examples from WMGStereo-150k achieve

Dataset	Middlebury-Train		DrivingStereo	
	2px	EPE	3px	EPE
DLNR-Sceneflow	24.23	18.49	18.65	4.79
DLNR-CREStereo	22.07	9.30	8.21	1.62
DLNR-IRS	16.36	7.21	3.89	1.06
DLNR-TartanAir	23.15	13.01	2.40	0.86
DLNR-Mixed	16.25	5.94	2.74	0.90
DLNR-FSD	<u>14.23</u>	<u>5.43</u>	2.59	0.89
DLNR-WMGStereo-150k	12.61	4.54	1.89	0.82

Table 6. **Zero-shot performance by dataset on held-out benchmarks** Training DLNR on WMGStereo-150k results in better performance on benchmarks not used in parameter adjustment, demonstrating our findings generalize to unseen scenarios.

a lower EPE than 100k CREStereo samples. Moreover, our procedural “recipe” continues to scale well as the number of training examples increases to over 100k samples, while SceneFlow plateaus at around 1000 samples and CREStereo at 10000 samples. Our dataset converges to a similar error as FSD, and demonstrates competitive sample efficiency.

5. Conclusion

In this work, we contribute a thorough study on *what matters in stereo dataset generation*. By carefully selecting the best design choices, we generate a new synthetic dataset and demonstrate that training solely on this dataset achieves stronger zero-shot performance than training on many widely used datasets combined. We believe that our study and open-source codebase will be continually useful for stereo matching research, especially in co-developing training data with new architectures.

6. Acknowledgments

This work was partially supported by the National Science Foundation and an Amazon Research Award.

References

[1] Wei Bao, Wei Wang, Yuhua Xu, Yulan Guo, Siyu Hong, and Xiaohu Zhang. Instereo2k: a large real dataset for stereo matching in indoor scenes. *Science China Information Sciences*, 63:1–11, 2020. 7

[2] Luca Bartolomei, Fabio Tosi, Matteo Poggi, and Stefano Mattoccia. Stereo anywhere: Robust zero-shot deep stereo matching even where either stereo or mono fail, 2025. 1, 5

[3] Daniel J Butler, Jonas Wulff, Garrett B Stanley, and Michael J Black. A naturalistic open source movie for optical flow evaluation. In *Computer Vision—ECCV 2012: 12th European Conference on Computer Vision, Florence, Italy, October 7–13, 2012, Proceedings, Part VI 12*, pages 611–625. Springer, 2012. 2

[4] Yohann Cabon, Naila Murray, and Martin Humenberger. Virtual kitti 2. *arXiv preprint arXiv:2001.10773*, 2020. 1, 2

[5] Jia-Ren Chang and Yong-Sheng Chen. Pyramid stereo matching network. In *Proceedings of the IEEE Conference on Computer Vision and Pattern Recognition*, pages 5410–5418, 2018. 1, 5

[6] Blender Online Community. *Blender - a 3D modelling and rendering package*. Blender Foundation, Stichting Blender Foundation, Amsterdam, 2018. 3

[7] Matt Deitke, Eli VanderBilt, Alvaro Herrasti, Luca Weihs, Jordi Salvador, Kiana Ehsani, Winson Han, Eric Kolve, Ali Farhadi, Aniruddha Kembhavi, and Roozbeh Mottaghi. ProcTHOR: Large-Scale Embodied AI Using Procedural Generation. In *NeurIPS, 2022*. Outstanding Paper Award. 3

[8] A. Dosovitskiy, P. Fischer, E. Ilg, P. Häusser, C. Hazırbaş, V. Golkov, P. v.d. Smagt, D. Cremers, and T. Brox. FlowNet: Learning optical flow with convolutional networks. In *IEEE International Conference on Computer Vision (ICCV)*, 2015. 3

[9] Adrien Gaidon, Qiao Wang, Yohann Cabon, and Eleonora Vig. Virtual worlds as proxy for multi-object tracking analysis. In *Proceedings of the IEEE conference on computer vision and pattern recognition*, pages 4340–4349, 2016. 1, 2

[10] Andreas Geiger, Philip Lenz, and Raquel Urtasun. Are we ready for autonomous driving? the kitti vision benchmark suite. In *2012 IEEE conference on computer vision and pattern recognition*, pages 3354–3361. IEEE, 2012. 4

[11] Klaus Greff, Francois Belletti, Lucas Beyer, Carl Doersch, Yilun Du, Daniel Duckworth, David J Fleet, Dan Gnanaprasam, Florian Golemo, Charles Herrmann, Thomas Kipf, Abhijit Kundu, Dmitry Lagun, Issam Laradji, Hsueh-Ti (Derek) Liu, Henning Meyer, Yishu Miao, Derek Nowrouzezahrai, Cengiz Oztireli, Etienne Pot, Noha Radwan, Daniel Rebain, Sara Sabour, Mehdi S. M. Sajjadi, Matan Sela, Vincent Sitzmann, Austin Stone, Deqing Sun, Suhani Vora, Ziyu Wang, Tianhao Wu, Kwang Moo Yi, Fangcheng Zhong, and Andrea Tagliasacchi. Kubric: a scalable dataset generator. 2022. 3

[12] Tongfan Guan, Chen Wang, and Yun-Hui Liu. Neural markov random field for stereo matching, 2024. 1, 5

[13] Hsin-Ping Huang, Charles Herrmann, Junhwa Hur, Erika Lu, Kyle Sargent, Austin Stone, Ming-Hsuan Yang, and Deqing Sun. Self-supervised autoflow. In *CVPR, 2023*. 3

[14] E. Ilg, T. Saikia, M. Keuper, and T. Brox. Occlusions, motion and depth boundaries with a generic network for disparity, optical flow or scene flow estimation. In *European Conference on Computer Vision (ECCV)*, 2018. 3

[15] Junpeng Jing, Ye Mao, Anlan Qiu, and Krystian Mikolajczyk. Match stereo videos via bidirectional alignment. 2024. 3

[16] Nikita Karaev, Ignacio Rocco, Benjamin Graham, Natalia Neverova, Andrea Vedaldi, and Christian Rupprecht. Dynamicstereo: Consistent dynamic depth from stereo videos. In *Proceedings of the IEEE/CVF Conference on Computer Vision and Pattern Recognition (CVPR)*, pages 13229–13239, 2023. 2

[17] Jiankun Li, Peisen Wang, Pengfei Xiong, Tao Cai, Ziwei Yan, Lei Yang, Jiangyu Liu, Haoqiang Fan, and Shuaicheng

- Liu. Practical stereo matching via cascaded recurrent network with adaptive correlation, 2022. 1, 2
- [18] Lahav Lipson, Zachary Teed, and Jia Deng. Raft-stereo: Multilevel recurrent field transforms for stereo matching. In *International Conference on 3D Vision (3DV)*, 2021. 4, 5, 8
- [19] Nikolaus Mayer, Eddy Ilg, Philip Hausser, Philipp Fischer, Daniel Cremers, Alexey Dosovitskiy, and Thomas Brox. A large dataset to train convolutional networks for disparity, optical flow, and scene flow estimation. In *Proceedings of the IEEE conference on computer vision and pattern recognition*, pages 4040–4048, 2016. 1, 2
- [20] Nikolaus Mayer, Eddy Ilg, Philipp Fischer, Caner Hazirbas, Daniel Cremers, Alexey Dosovitskiy, and Thomas Brox. What makes good synthetic training data for learning disparity and optical flow estimation? *International Journal of Computer Vision*, 126(9):942–960, 2018. 3, 4, 7
- [21] Lukas Mehl, Jenny Schmalfluss, Azin Jahedi, Yaroslava Nalivayko, and Andrés Bruhn. Spring: A high-resolution high-detail dataset and benchmark for scene flow, optical flow and stereo. In *Proc. IEEE/CVF Conference on Computer Vision and Pattern Recognition (CVPR)*, 2023. 2
- [22] Moritz Menze and Andreas Geiger. Object scene flow for autonomous vehicles. In *Proceedings of the IEEE conference on computer vision and pattern recognition*, pages 3061–3070, 2015. 4
- [23] Alexander Raistrick, Lahav Lipson, Zeyu Ma, Lingjie Mei, Mingzhe Wang, Yiming Zuo, Karhan Kayan, Hongyu Wen, Beining Han, Yihan Wang, Alejandro Newell, Hei Law, Ankit Goyal, Kaiyu Yang, and Jia Deng. Infinite photorealistic worlds using procedural generation. In *Proceedings of the IEEE/CVF Conference on Computer Vision and Pattern Recognition*, pages 12630–12641, 2023. 1, 3
- [24] Alexander Raistrick, Lingjie Mei, Karhan Kayan, David Yan, Yiming Zuo, Beining Han, Hongyu Wen, Meenal Parakh, Stamatis Alexandropoulos, Lahav Lipson, Zeyu Ma, and Jia Deng. Infinigen indoors: Photorealistic indoor scenes using procedural generation. In *Proceedings of the IEEE/CVF Conference on Computer Vision and Pattern Recognition (CVPR)*, pages 21783–21794, 2024. 1, 3
- [25] Pierluigi Zama Ramirez, Alex Costanzino, Fabio Tosi, Matteo Poggi, Samuele Salti, Stefano Mattoccia, and Luigi Di Stefano. Booster: A benchmark for depth from images of specular and transparent surfaces. *IEEE Transactions on Pattern Analysis and Machine Intelligence*, 46(1):85–102, 2024. 2, 4, 7
- [26] Daniel Scharstein, Heiko Hirschmüller, York Kitajima, Gökhan Krathwohl, Nera Nešić, Xiang Wang, and Peter Westling. High-resolution stereo datasets with subpixel-accurate ground truth, 2014. 2, 4
- [27] Thomas Schöps, Johannes L. Schönberger, Silvano Galliani, Torsten Sattler, Konrad Schindler, Marc Pollefeys, and Andreas Geiger. A multi-view stereo benchmark with high-resolution images and multi-camera videos. In *Conference on Computer Vision and Pattern Recognition (CVPR)*, 2017. 4
- [28] Deqing Sun, Daniel Vlasic, Charles Herrmann, Varun Jampani, Michael Krainin, Huiwen Chang, Ramin Zabih, William T Freeman, and Ce Liu. Autoflow: Learning a better training set for optical flow. In *CVPR*, 2021. 3
- [29] Fabio Tosi, Yiyi Liao, Carolin Schmitt, and Andreas Geiger. Smd-nets: Stereo mixture density networks. *CoRR*, abs/2104.03866, 2021. 2
- [30] Jonathan Tremblay, Thang To, and Stan Birchfield. Falling things: A synthetic dataset for 3d object detection and pose estimation. In *Proceedings of the IEEE Conference on Computer Vision and Pattern Recognition Workshops*, pages 2038–2041, 2018. 1, 2
- [31] Qiang Wang, Shizhen Zheng, Qingsong Yan, Fei Deng, Kaiyong Zhao, and Xiaowen Chu. Irs: A large naturalistic indoor robotics stereo dataset to train deep models for disparity and surface normal estimation. In *2021 IEEE International Conference on Multimedia and Expo (ICME)*, pages 1–6. IEEE, 2021. 2
- [32] Wenshan Wang, Delong Zhu, Xiangwei Wang, Yaoyu Hu, Yuheng Qiu, Chen Wang, Yafei Hu, Ashish Kapoor, and Sebastian Scherer. Tartanair: A dataset to push the limits of visual slam, 2020. 1, 2
- [33] Xianqi Wang, Gangwei Xu, Hao Jia, and Xin Yang. Selective-stereo: Adaptive frequency information selection for stereo matching. In *Proceedings of the IEEE/CVF Conference on Computer Vision and Pattern Recognition*, pages 19701–19710, 2024. 1, 5, 8
- [34] Yingqian Wang, Longguang Wang, Jungang Yang, Wei An, and Yulan Guo. Flickr1024: A large-scale dataset for stereo image super-resolution. In *Proceedings of the IEEE/CVF International Conference on Computer Vision Workshops*, pages 0–0, 2019. 7
- [35] Philippe Weinzaepfel, Thomas Lucas, Vincent Leroy, Johann Cabon, Vaibhav Arora, Romain Brégier, Gabriela Csurka, Leonid Antsfeld, Boris Chidlovskii, and Jérôme Revaud. CroCo v2: Improved Cross-view Completion Pre-training for Stereo Matching and Optical Flow. In *ICCV*, 2023. 1
- [36] Bowen Wen, Matthew Trepte, Joseph Aribido, Jan Kautz, Orazio Gallo, and Stan Birchfield. Foundationstereo: Zero-shot stereo matching, 2025. 1, 2, 5
- [37] Gangwei Xu, Xianqi Wang, Xiaohuan Ding, and Xin Yang. Iterative geometry encoding volume for stereo matching, 2023. 1, 5
- [38] Gangwei Xu, Xianqi Wang, Zhaoxing Zhang, Junda Cheng, Chunyuan Liao, and Xin Yang. Igev++: Iterative multi-range geometry encoding volumes for stereo matching. *arXiv preprint arXiv:2409.00638*, 2024. 1, 5
- [39] Haofei Xu, Jing Zhang, Jianfei Cai, Hamid Rezatofghi, Fisher Yu, Dacheng Tao, and Andreas Geiger. Unifying flow, stereo and depth estimation. *IEEE Transactions on Pattern Analysis and Machine Intelligence*, 2023. 5
- [40] Gengshan Yang, Joshua Manela, Michael Happold, and Deva Ramanan. Hierarchical deep stereo matching on high-resolution images. In *Proceedings of the IEEE/CVF Conference on Computer Vision and Pattern Recognition*, pages 5515–5524, 2019. 1, 2
- [41] Guorun Yang, Xiao Song, Chaoqin Huang, Zhidong Deng, Jianping Shi, and Bolei Zhou. Drivingstereo: A large-scale

- dataset for stereo matching in autonomous driving scenarios. In *Proceedings of the IEEE/CVF Conference on Computer Vision and Pattern Recognition (CVPR)*, 2019. 8
- [42] Lihe Yang, Bingyi Kang, Zilong Huang, Zhen Zhao, Xiaogang Xu, Jiashi Feng, and Hengshuang Zhao. Depth anything v2, 2024. 8
- [43] Zhichao Yin, Trevor Darrell, and Fisher Yu. Hierarchical discrete distribution decomposition for match density estimation. In *Proceedings of the IEEE/CVF conference on computer vision and pattern recognition*, pages 6044–6053, 2019. 1
- [44] Jiayi Zeng, Chengtang Yao, Yuwei Wu, and Yunde Jia. Temporally consistent stereo matching. In *Proceedings of the European Conference on Computer Vision (ECCV)*, 2024.
- [45] Haoliang Zhao, Huizhou Zhou, Yongjun Zhang, Jie Chen, Yitong Yang, and Yong Zhao. High-frequency stereo matching network. In *Proceedings of the IEEE/CVF Conference on Computer Vision and Pattern Recognition*, pages 1327–1336, 2023. 1, 2, 5, 8

Appendix

A. Additional Analysis

Parameter Study In Tab. 7, we provide an additional standard metric, end-point-error (EPE), for the same parameter study experiments in the main paper. For most benchmarks and experiments, the best model by px accuracy is also the best by EPE, demonstrating the robustness of our results.

B. Additional Generation Details

B.1. Indoor Floating Objects Scene Type

For each scene, we first generate the indoor scene using our modified Infinigen Indoors settings. Given this indoor scene, we place the random objects in the scene, respecting collisions with existing scene objects. We then place the 20 camera rigs using the default Infinigen Indoors placement algorithm, which attempts to maximize the standard deviation of depth values. Finally, we apply augmentations as described in Section 3. We randomize the materials of all floating and background objects, replacing an object’s default material with a randomly chosen material with probability 0.5. To account for the large variance in object sizes, we normalize the floating object sizes.

B.2. Dense Floating Objects Scene Type

For each scene, we first spawn 200 objects into a scene at the origin, and use Blender’s key-frame animation system to assign each object different locations, orientation, etc. at every single keyframe. Objects were placed at a distance sampled from Uniform[5,50] m away from the camera and the camera baselines were sampled from Uniform[0.1, 0.4] m. Similar to indoor scenes, we place point lights at random distances and normalize floating object size. We rescale object size based on distance to prevent far-away objects from being completely occluded by nearby objects and apply random warping to objects. We also perform additional lighting augmentations, randomizing the sky background’s strength and color.

B.3. Nature Scene Type

We generate nature scenes with the Infinigen Nature system, using default configurations unless otherwise specified in this section and 3. By default, the Infinigen system provides configurations to render videos from a camera trajectory placed within a scene. However, these video sequences have high amounts of overlap between consecutive frames, so we render videos from camera trajectories at 6 frames per second to reduce similarity between consecutive frames. We render 50 frames from each video and sample the baseline of the stereo rig from Uniform[0.075, 0.5].

B.4. Ground Truth

For all frames, we provide camera intrinsics and extrinsics, left and right depth maps, and occlusion maps. We convert depth maps to disparity using the camera intrinsics and extrinsics. We compute occlusion maps by checking left-to-right and right-to-left re-projection consistency, with a 1 percent difference threshold. We also provide object segmentation maps, where each pixel has a value associated with an object’s index value. Because procedural objects are never reused, we provide object names associated with each index, which enables the creation of flexible semantic segmentation maps. Similarly, materials are also procedural and never reused, so we provide material segmentation maps with material names. All frames are rendered at 1280 x 720 resolution.

B.5. Dataset post-processing

Certain types of undesirable scenes are hard to prevent during dataset generation, so we provide tools to remove them as a post-processing step. We use a simple mean of pixel intensities to filter out frames that are extremely dark as a result of lighting augmentation. We remove all frames with any depth value lower than a certain threshold to eliminate scenarios where the camera clips into an object or when an object has extremely large disparity values. This threshold is set to 12.5 cm for indoor scenes and 5 m for nature scenes.

B.6. Atmospheric effects

We disable rain, dust, and snow particles from generation because they produce depth values that are almost invisible in rendered images. Similarly, we disable the coral reef scene type because of insufficiently visible background objects.

B.7. List of Assets Used

ArmChair	Balloon
BarChair	BasketBase
Bathtub	BathroomSink
Bed	BedFrame
BeverageFridge	Blanket
BookColumn	Book
BookStack	Bottle
Bowl	Can
CeilingClassicLamp	CellShelf
Chair	Chopsticks
Cup	CurvedStaircase
DeskLamp	Dishwasher
FloorLamp	FoodBag
FoodBox	Fork
GlassPanelDoor	Hardware
Jar	KitchenCabinet
KitchenIsland	KitchenSpace
Knife	Lamp
LargePlantContainer	LargeShelf
Lid	LiteDoor
LouverDoor	Mattress
Microwave	Monitor
NatureShelfTrinkets	OfficeChair
Oven	Pallet
Pants	PanelDoor
Pillow	PlantContainer
Plate	Pot
Rug	Shirt
SimpleBookcase	SimpleDesk
Sink	SingleCabinet
Sofa	SpiralStaircase
Spoon	StraightStaircase
TableCocktail	TableDining
Tap	Towel
TriangleShelf	TV
TVStand	Vase
WallArt	Wineglass
UShapedStaircase	

Experiment	Method	Middlebury 2014				Middlebury 2021		ETH3D		KITTI				Booster (Q)	
		H		F		-		-		2012		2015		-	
		px	EPE	px	EPE	px	EPE	px	EPE	px	EPE	px	EPE	px	EPE
Floating Object Density	No floating Objects	12.52	3.91	18.44	12.13	16.31	3.29	4.47	0.36	4.42	0.93	6.19	1.20	16.40	4.14
	0 to 10 floating objects	7.78	2.19	11.42	5.28	11.30	1.66	3.62	0.31	4.44	0.91	6.09	1.15	12.21	2.64
	10 to 30 floating objects	6.60	1.77	9.19	4.37	10.28	1.55	3.92	0.30	4.05	0.86	5.11	1.05	10.60	2.20
Background Objects	No background objects	8.35	2.15	10.42	5.58	12.01	1.68	4.39	0.35	4.20	0.92	6.28	1.21	12.72	3.34
	With background objects	6.60	1.77	9.19	4.37	10.28	1.55	3.92	0.30	4.05	0.86	5.11	1.05	10.60	2.20
Floating Object Type	Floating chairs	5.29	1.50	9.24	5.84	9.81	1.41	3.64	0.29	4.90	1.01	7.02	1.22	11.22	2.71
	Floating shelves	7.13	1.89	10.28	5.05	10.24	1.43	3.51	0.31	4.32	0.94	6.06	1.16	11.63	2.31
	Floating bushes	6.04	1.48	9.21	3.83	9.54	1.40	3.13	0.28	3.86	0.86	5.42	1.11	12.19	2.72
	All generators used	6.60	1.77	9.19	4.37	10.28	1.55	3.92	0.30	4.05	0.86	5.11	1.05	10.60	2.20
Object Material	No materials	9.02	2.32	11.42	6.37	10.65	1.56	3.48	0.32	4.34	0.93	6.07	1.18	14.07	3.67
	One diffuse material	7.21	1.82	10.09	5.28	9.65	1.43	2.77	0.29	3.76	0.84	5.41	1.09	12.73	3.62
	Only metal and glass	8.37	2.06	11.28	6.47	11.85	1.73	4.95	0.34	4.06	0.86	4.97	1.04	9.80	1.60
	All materials used	6.60	1.77	9.19	4.37	10.28	1.55	3.92	0.30	4.05	0.86	5.11	1.05	10.60	2.20
Stereo Baseline	Uniform[0.04, 0.1]	9.60	4.03	32.47	33.02	22.18	14.70	2.89	0.27	5.13	1.05	6.64	1.22	17.03	5.22
	Uniform[0.2, 0.3]	7.01	2.17	9.75	5.39	10.50	1.72	14.05	6.00	3.94	0.86	5.37	1.10	8.96	1.76
	Uniform[0.04, 0.4]	6.60	1.77	9.19	4.37	10.28	1.55	3.92	0.30	4.05	0.86	5.11	1.05	10.60	2.20
Lighting	Realistic Lighting	6.91	1.74	9.62	4.36	10.06	1.46	3.81	0.31	3.95	0.88	5.45	1.10	10.45	2.09
	Augmented Lighting	6.60	1.77	9.19	4.37	10.28	1.55	3.92	0.30	4.05	0.86	5.11	1.05	10.60	2.20

Table 7. **Expanded metrics for parameter study.** We compute EPE on all valid pixels.

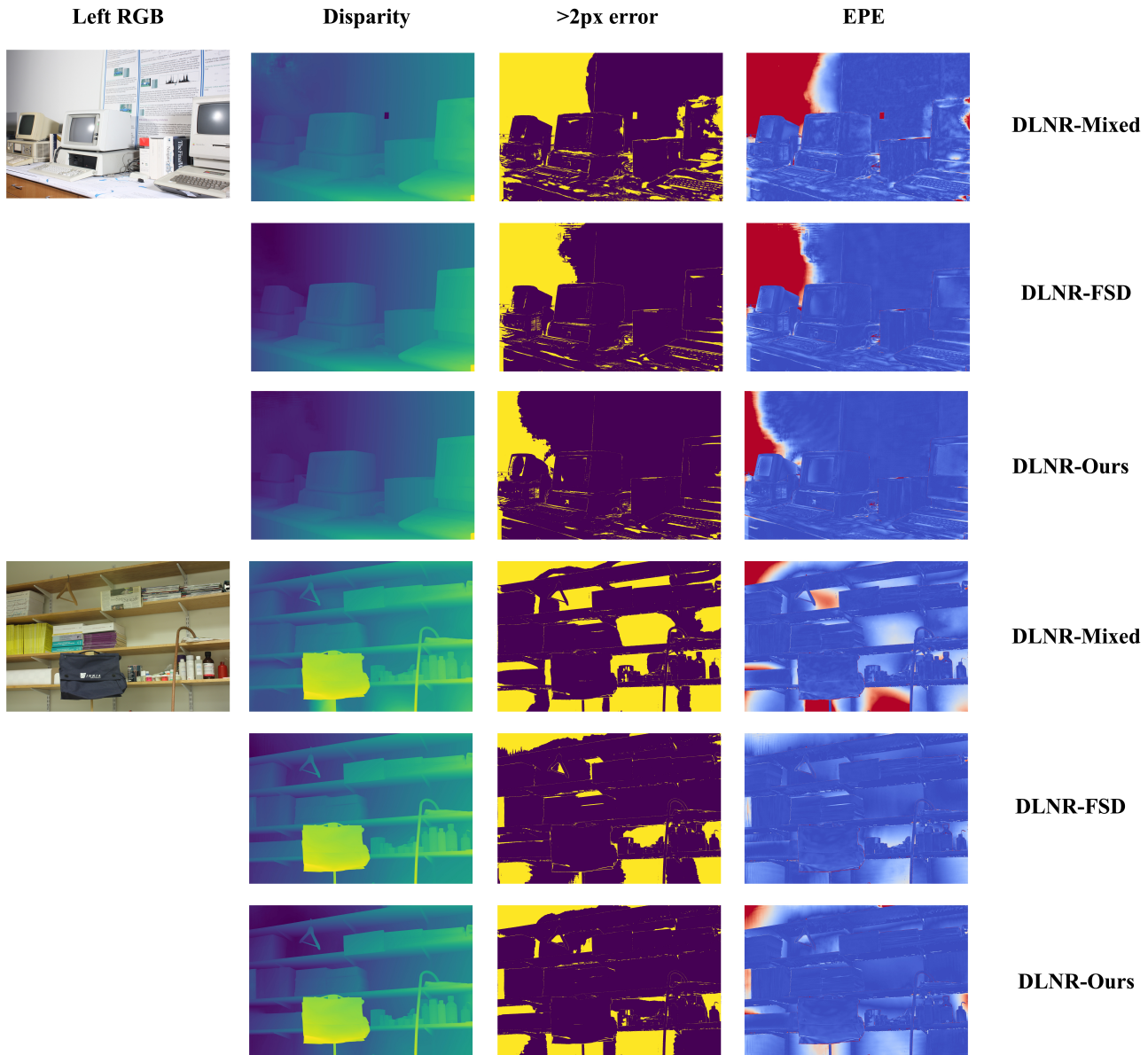


Figure 6. Qualitative results comparing DLNR-WMGStereo-150k, DLNR-FSD, and DLNR-Mixed on the 2014 Middlebury Eval set. Training on our dataset results in more accurate capture of walls and textureless regions than DLNR-Mixed and comparable performance with DLNR-FSD.

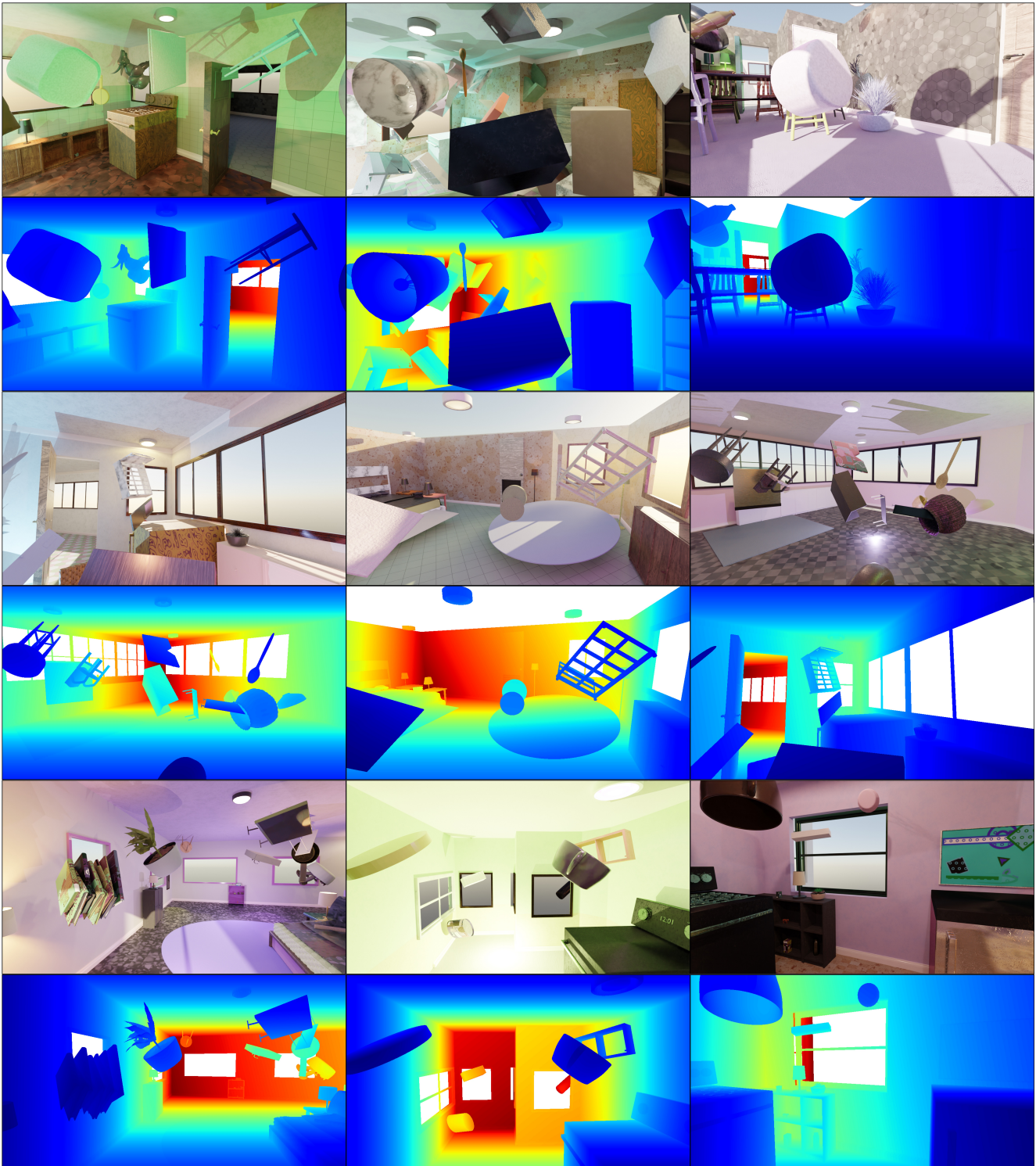


Figure 7. Non-cherry-picked, random samples from our floating indoor dataset type. We remove the glass portion of the window mesh entirely, instead of replacing the material, in order to maintain good lighting, as specified in Section 3. This modification is a configurable option, and new data can be generated with the window meshes in place.

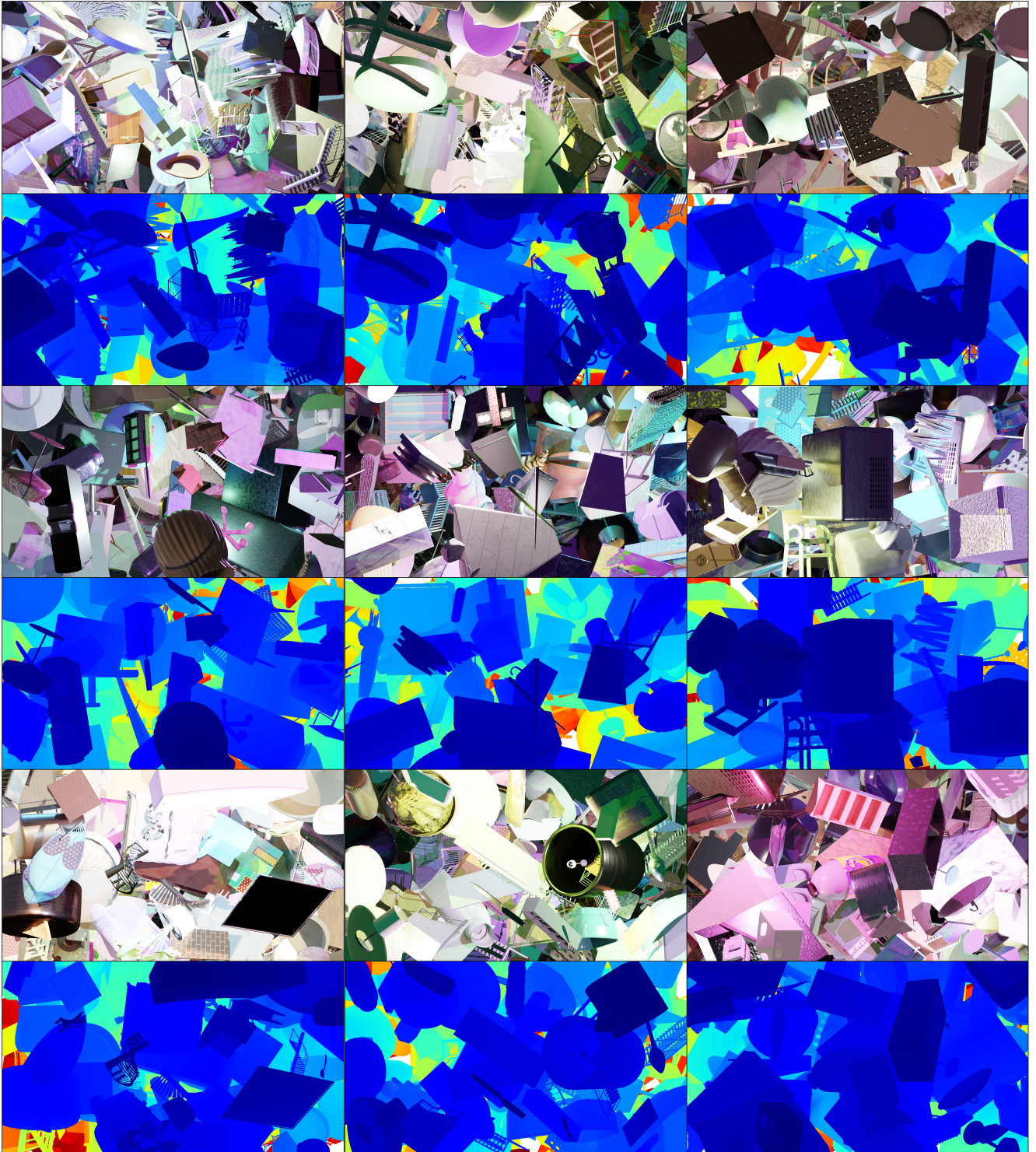


Figure 8. Non-cherry-picked, random samples from our dense floating dataset type.

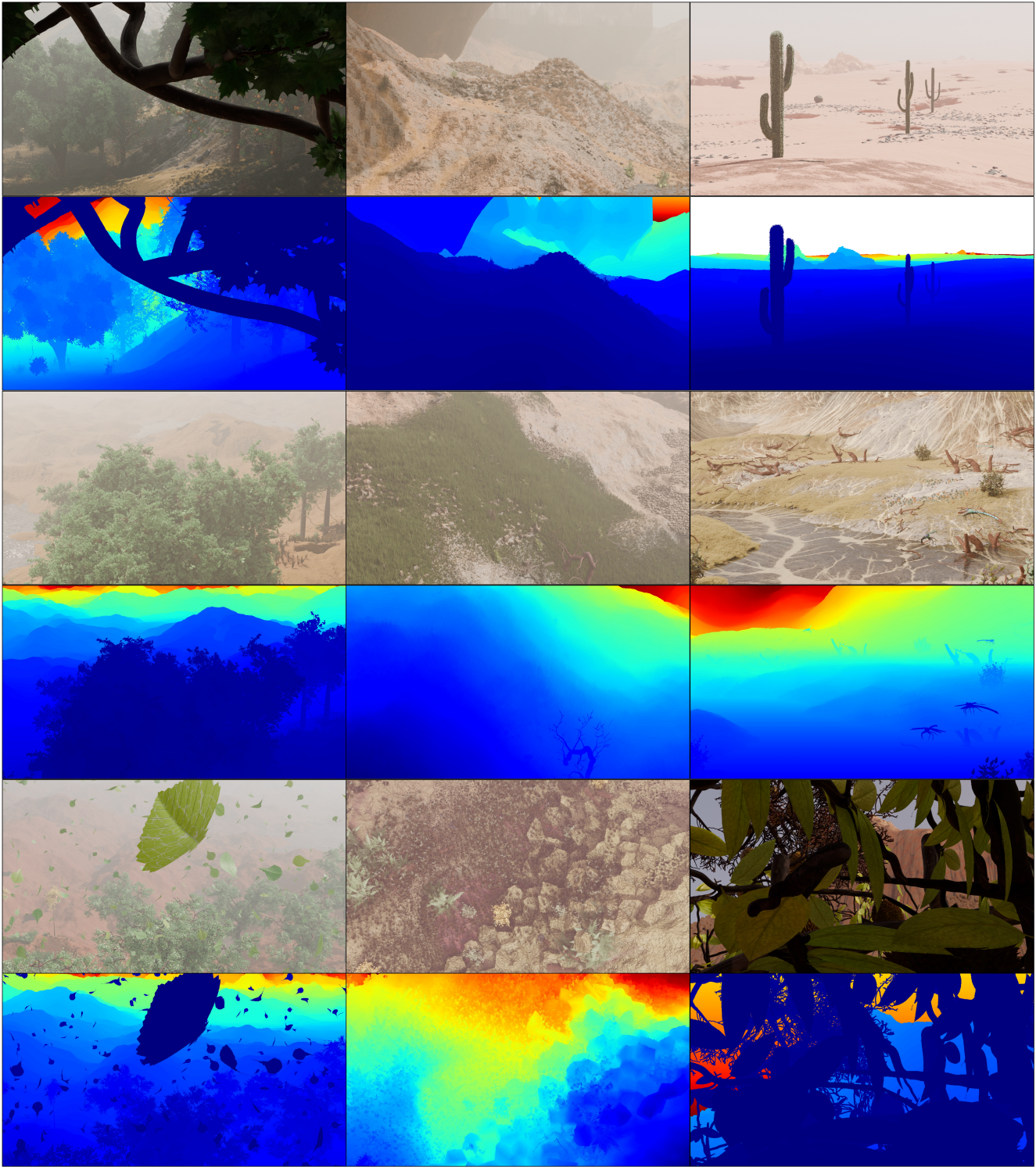


Figure 9. Non-cherry-picked, random samples from our nature dataset type.